Charging effects during focused electron beam induced deposition of silicon oxide

de Boer, Sanne K.; van Dorp, Willem F.; De Hosson, Jeff Th. M.

Published in:
Journal of Vacuum Science & Technology B

DOI:
10.1116/1.3659713

Publication date:
2011

Charging effects during focused electron beam induced deposition of silicon oxide

Sanne K. de Boer, Willem F. van Dorp,[a] and Jeff Th. M. De Hosson
University of Groningen, Zernike Institute for Advanced Materials, Department of Applied Physics, Nijenborgh 4, 9747 AG Groningen, the Netherlands

(Received 22 June 2011; accepted 15 October 2011; published 8 November 2011)

This paper concentrates on focused electron beam induced deposition of silicon oxide. Silicon oxide pillars are written using 2, 4, 6, 8, 10-pentamethyl-cyclopenta-siloxane (PMCPS) as precursor. It is observed that branching of the pillar occurs above a minimum pillar height. The branching is attributed to charging of the deposit by the electron beam. The branching can be suppressed by introducing water into the chamber together with PMCPS. At the same time, the cointroduction of water results in a higher growth rate, which is found to be specific to PMCPS. © *2011 American Vacuum Society*. [DOI: 10.1116/1.3659713]

I. INTRODUCTION

Focused electron beam induced deposition (FEBID) is a prototyping and lithography technique that uses an electron beam to dissociate gaseous, adsorbed precursor molecules.[1–5] FEBID is typically done with a scanning electron microscope or dual beam instrument, but can be done in a transmission electron microscope (TEM) as well. A gaseous precursor is introduced in the electron microscope, usually through a nozzle which directs the gas flow to the sample. The precursor molecules, carrying the material that one wants to deposit, adsorb on the sample surface and the molecules are cracked under the influence of electrons. The nonvolatile fragments form the pattern and the volatile fragments are removed by the vacuum system.

An economically important application of FEBID is mask repair for optical lithography.[6,7] The use of the electron beam makes it possible to modify UV and EUV masks damage-free; in contrast to, for instance, the use of gallium ion beams which always involves incorporating Ga^+ ions in the target. Other applications of FEBID are the fabrication of probes for scanning probe microscopy,[8] nanomanipulators,[9] and electrical contacts.[10]

As microtechnology and nanotechnology develop, FEBID promises to be of increasing importance. Since borders between physics, chemistry, and biology become increasingly diffuse, a need develops for a fabrication technique that is accessible, versatile and flexible. At the same time, it is challenging to continue the trend for miniaturization to below 10 nm with mainstream lithography techniques. FEBID allows for both direct-write 3D prototyping[11] and lithography in the sub-10 nm regime.[12–14]

Silicon oxide is among the materials that can be deposited with FEBID. The ability to locally deposit insulating materials is not only relevant for mask repair such as described earlier,[15–17] but also for circuit rewiring and repair[18,19] or for use as an etch mask for further processing.[20] In this paper, we report the results of our study of the growth of silicon oxide pillars.

[a]Electronic mail: w.f.van.dorp@rug.nl

II. EXPERIMENT

The patterning and imaging is done with a Tescan Lyra dual beam instrument operated at 30 keV, equipped with a Schottky emitter. Prior to all deposition experiments, the sample chamber, including the mounted sample, is plasma cleaned for 16 h. The cleaner is an Evactron decontaminator that uses air to generate the plasma. The substrates are n-type doped Si with a resistivity of 0.005 Ω cm and 200 nm thick holey silicon nitride membranes. The precursors used in this study are 2, 4, 6, 8, 10-pentamethyl-cyclopenta-siloxane (PMCPS, CAS 6166-86-5) for silicon oxide patterning, tungsten hexacarbonyl ($W(CO)_6$, CAS 14040-11-0) for the deposition of tungsten containing material and water. All gases are introduced into the microscope using a factory-installed five-needle gas injection system. To some extent, the precursor flux can be varied by changing the distance between nozzle and sample. The beam current used in the experiments is between 500 pA and 2 nA, which is measured using a Faraday cup. The background pressure is 2×10^{-5} mbar.

Elemental analysis is performed with a Bruker Quantax energy-dispersive spectroscopy (EDS) analyzer on a Jeol 2010F transmission electron microscope operated at 200keV. Atomic force microscopy measurements for height measurements are performed with a Nanoscope IIIa.

III. RESULTS AND DISCUSSION

Figure 1(a) shows an array of pillars that are written using PMCPS as precursor. The pillars are written serially, moving to the next position only after completing the exposure of the first position. Here we define the dwell time as the total time that each position is irradiated by the beam. For all pillars it is observed that branching occurs. On top of a smooth stem, each pillar shows many branches. Some of the pillars are bent; this most likely due to proximity effects.[21] Figure 1(b) shows a second array, written with a dwell time of 9 s per pillar and a lower precursor flux. The lower precursor flux was achieved by positioning the gas nozzle further away from the sample. Again branching occurs for all pillars.

Deposits written with PMCPS are analyzed by EDS. The deposits are written on a copper supported lacey carbon

TEM grid. During the EDS measurements, care was taken not to include the supporting carbon in the measurement of the silicon oxide composition. The composition was found to be $SiO_{1.1}C_{0.06}$, with a quantification error of 5 at. %.

The branching effect as well as the height at which it occurs are reproducible. In Fig. 2(a) silicon oxide pillars are shown, grown with increasing dwell times from 35 ms (left bottom) to 3.4 s (right top) and a beam current of 500 pA. While the lower pillars are smooth and cone-shaped, all higher pillars consistently show branching starting at a height of about 800 nm. The same pattern is shown in Fig. 2(b), but now written with a beam current of 1.6 nA. The total electron dose per pillar was the same as for the pillars in Fig. 3(a). We have observed that the branching also occurs when a beam current of 40 pA is used.

When we use a 200 nm thick (insulating) SiN membrane as substrate instead of a (conducting) Si wafer, we observe similar branching of the deposits. The arrays of deposits in Fig. 3(a) are written with dwell times increasing from 30 s (left) to 73 s (right), with a constant dwell time per array. It is observed that branching occurs more extensively and directly from the start of the growth, without the formation of a smooth stem such as in Figs. 1 and 2. The bright field TEM images in Fig. 3(b) and 3(c) show deposits created by spot exposures of a few seconds close to an edge of the SiN sample, in the presence of PMCPS. The branches form in all directions and show no sign of crystallinity.

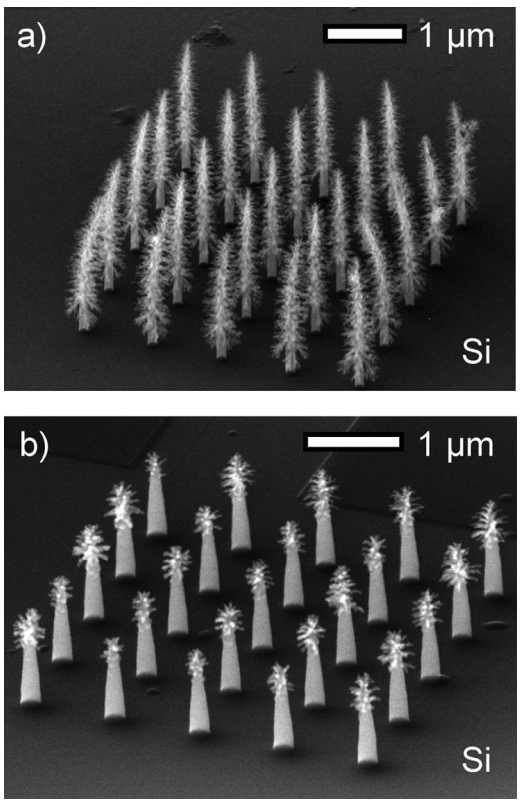

FIG. 1. (a) Array of silicon oxide pillars, written with 616 pA and a dwell time of 3 s per pillar. (b) Pillars written with 2 nA, a dwell time of 9 s per pillar, and a lower precursor flux. Branching is observed for all pillars. The bending of the pillars in (a) is most likely due to proximity effects.

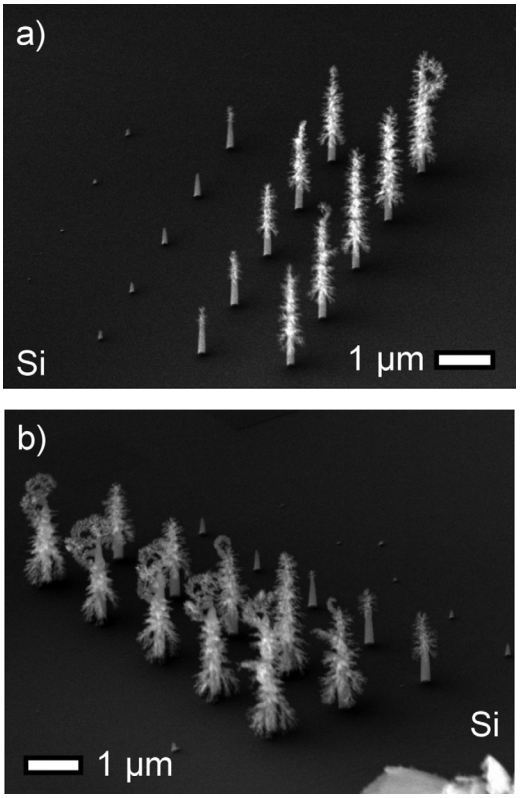

FIG. 2. (a) Series of silicon oxide pillars written with dwell times from 35 ms (left bottom) to 3.4 s (right top) and a beam current of 500 pA. (b) The same pattern, but now written from top right to bottom center with a beam current of 1.6 nA. The total electron dose per pillar was the same as in (a). The pillars are imaged at a tilt angle of 60°. Branching occurs at a constant pillar height of about 800 nm.

The branching of the silicon oxide deposits is consistent with charging effects that are reported for the electron beam induced growth of conducting deposits on insulating substrates. Over length scales ranging from tens of nanometers[22] to micrometers[23] treelike structures can form on (the edge of) an insulating sample under the influence of intense electron radiation. Banhart suggests that the build-up of charge on the sample causes precursor molecules to follow deterministic instead of ballistic trajectories.[24] The electric field that is the created by the accumulated charge either ionizes or polarizes precursor molecules, such as tungsten hexacarbonyl[22] or hydrocarbons,[23] and draws them towards the irradiated spot.

If charging plays a role in our experiments, the silicon oxide pillars will be positively charged. During the electron irradiation of any sample, there is a balance between the incident primary electrons (PEs) and the emitted secondary electrons (SEs). An insulating sample can become positively or negatively charged, depending on the SE yield of the irradiated material at the given PE energy. For planar SiO_2 at zero-tilt incidence the SE yield at a PE energy of 30 keV is well below unity,[25] which would suggest negative charging (more electrons are injected into the sample as PEs than emitted as SEs). However, SE emission from the near-vertical sidewalls of the growing silicon oxide pillars leads to a net loss of electrons,[26] so that positive charging will result. Modeling the

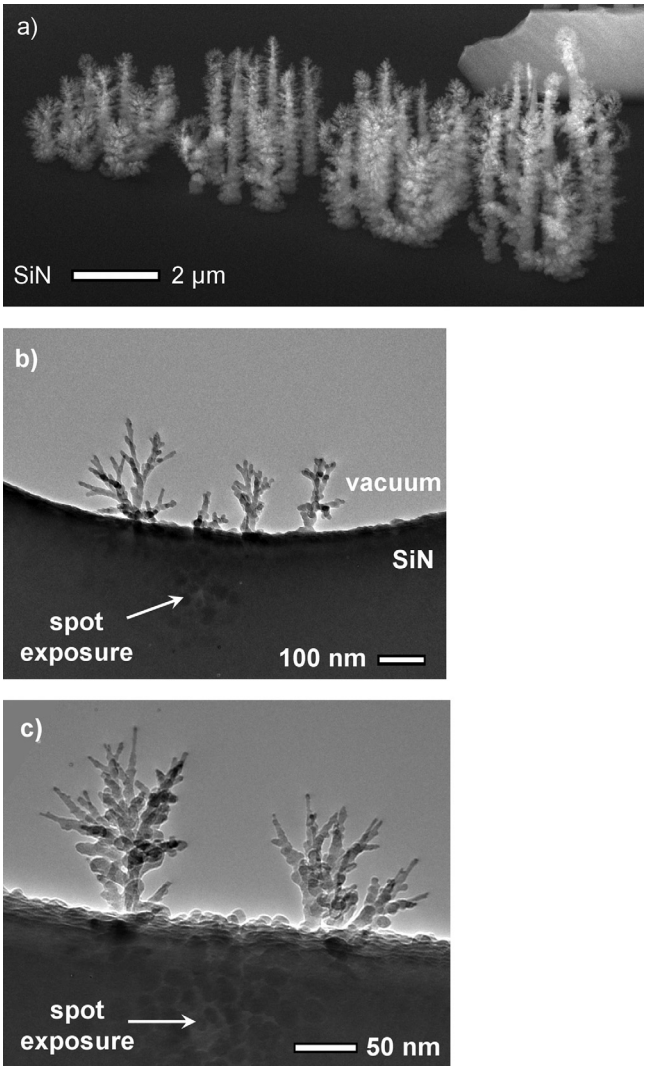

FIG. 3. (a) Arrays of deposits written on a SiN membrane with dwell times increasing from 30 s (left) to 73 s (right) and a beam current of 509 pA. Bright field TEM images (b),(c) show deposits created by a spot exposure of a few seconds in the presence of PMCPS. The location of the spot exposure is indicated.

height at which the branching occurs is complex, mostly because it is unknown at what potential the precursor molecules are ionized or sufficiently polarized to induce the branching. In addition, the shape of the deposit changes during growth, as well as the size of the interaction volume of the scattering electrons. Finally, the deposit may not be an ideal insulator. Carbon, either from the residual gas or from the incomplete dissociation of ligand fragments, can be included in the deposit and may give a conduction path from deposit tip to substrate.

If the branching is indeed caused by the build-up of charge at the apex, the branching should be suppressed when water is introduced into the vacuum chamber together with PMCPS. It is known from environmental scanning electron microscopy that charge can be carried away from an insulating surface by ionized water.[27,28]

Figure 4 shows the results for the deposition of silicon oxide pillars in silicon during the cointroduction of water.

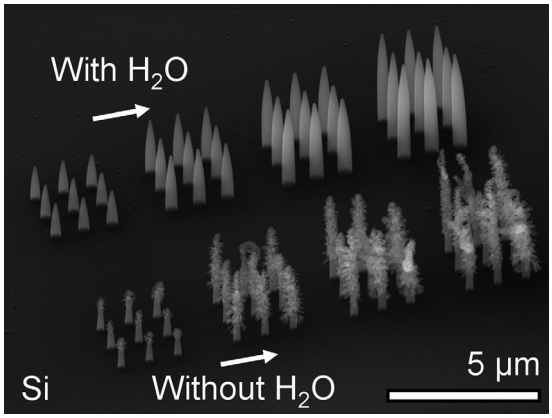

FIG. 4. Arrays of pillars are written on silicon with and without the cointroduction of water (upper and lower row, respectively). The dwell times increased from 16 s (left) to 39 s (right), the beam current is 514 pA. The presence of water prevents branching of the pillars.

Under identical conditions (dwell times, precursor pressure, etc.) the pillars written with the cointroduction of water have a smooth surface and show no branching. EDS measurements show that the cointroduction of water changes the composition from $SiO_{1.1}C_{0.06}$ to $SiO_{1.5}C_0$. The relative oxygen content is increased and the carbon content drops to below the detection limit. That charging is suppressed with the cointroduction of water while at the same time the carbon content is decreased, confirms the hypothesis that the branching is caused by charging of the deposit. A lower carbon content is expected to increase the resistivity of the silicon oxide, making charging more likely.

Apart from suppressing the branching, it is also observed in Fig. 4 that the growth rate is higher when cointroducing water. Although the pillars heights are difficult to compare in Fig. 4 due to the branching effect, pillars written in the presence of water have a considerably larger diameter. For a proper measurement of the difference in growth rate, 3 μm squares were deposited. The height of the squares was determined by AFM and the results are shown in Fig. 5. The silicon oxide growth rate is clearly higher in the presence of H_2O.

Since the PMCPS flux is not varied during the writing of the squares, the higher growth rate must be caused by the fact that more PMCPS molecules participate in the decomposition reactions if water is cointroduced. From sol-gel chemistry it is known that hydrolysis and condensation of siloxanes is possible in the presence of water, where the balance between hydrolysis and condensation depends on the *p*H of the solution.[29] For instance, tetraethyl-orthosilicate (TEOS) can react with water to form SiO_2, releasing ethanol. Our results suggest that the hydrolysis and/or the condensation can also be electron-induced, which is consistent with observations found by Perentes *et al.* They found evidence of TEOS and tetramethyl-orthosilicate (TMOS) reacting with residual water. In high vacuum systems water is always present as a residual gas, even without the intentional cointroduction. Perentes *et al.* observed an increase in FEBID growth rate when oxygen was cointroduced with TMOS and TEOS.[15,30]

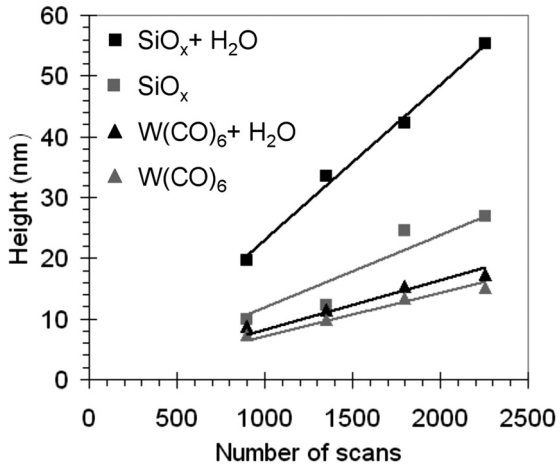

FIG. 5. Deposit height as function of the number of scans. Water increases the growth rate of silicon oxide deposits, while this effect is absent for tungsten-containing deposits. The deposits were written with a beam current of 2 nA, using a dwell time of 1 μs and beam step size of 3.5 nm.

Similarly, Mulders *et al.* found that water facilitates the decomposition of TEOS in FEBID experiments.[31]

To confirm that the effect of water on the growth rate is precursor-specific, we deposited identical squares with and without H_2O, using $W(CO)_6$. The results, plotted in Fig. 5, show that the water does not significantly affect the growth rate for $W(CO)_6$. This demonstrates that the effect is selective for PMCPS. It is also observed in Fig. 5 that, without the cointroduction of H_2O, the growth rate is higher for PMCPS than for $W(CO)_6$. This can be due to differences in gas flux, residence times of the precursor molecules on the surface, or dissociation cross sections. The difference can also be caused by water from the residual gas, which could enhance the growth of silicon oxide deposits.[15]

In this work, the precursor PMCPS is used to write insulating deposits on a conducting substrate. Branching of pillars may also occur when using other precursors to write insulating deposits, such as TEOS and TMOS (silicon oxide[15]), $Ti(NO_3)$ (titanium oxide[16]), and $Fe(CO)_5$ in combination of H_2O (iron oxide[32]). The findings in this paper may also be relevant to focused ion beam induced deposition (FIBID). Significantly more secondary electrons are generated per primary ion in FIBID than per primary electron in FEBID. This can possibly lead to significant charging effects if insulating precursors are used in FIBID.

IV. SUMMARY AND CONCLUSIONS

We used the precursor PMCPS for the deposition of $SiO_{1.1}C_{0.06}$ pillars. Above a pillar height of about 800 nm branching of the pillar is observed. The branching is attributed to charging at the apex of the insulating silicon oxide pillars. The branching can be suppressed by cointroducing water; smooth $SiO_{1.5}C_0$ pillars are obtained in the presence of water. A side effect of the cointroduction of water is a higher deposition rate of the silicon oxide. A comparison with the precursor $W(CO)_6$ shows that this effect is specific to PMCPS. The higher growth rate is attributed to the electron-induced hydrolysis of PMCPS during the cointroduction of water.

ACKNOWLEDGMENTS

The research is supported by a VENI grant through the Netherlands Organization for Research (NWO-the Hague, the Netherlands) and made possible by the Foundation for Technical Sciences (STW-Utrecht).

[1]I. Utke, P. Hoffman, and J. Melngailis, J. Vac. Sci. Technol. B **26**, 1197 (2008).
[2]S. J. Randolph, J. D. Fowlkes, and P. D. Rack, Crit. Rev. Solid State Mater. Sci. **31**, 55 (2006).
[3]K. Furuya, Sci. Technol. Adv. Mater. **9**, 014110 (2008).
[4]A. Botman, J. J. L. Mulders, and C. W. Hagen, Nanotechnology **20**, 372001 (2009).
[5]W. F. van Dorp and C. W. Hagen, J. Appl. Phys. **104**, 081301 (2008).
[6]T. Liang, E. Frendberg, B. Lieberman, and A. Stivers, J. Vac. Sci. Technol. B **23**, 3101 (2005).
[7]K. Edinger, H. Becht, J. Bihr, V. Boegli, M. Budach, T. Hofmann, H. W. P. Koops, P. Kuschnerus, J. Oster, P. Spies, and B. Weyrauch, J. Vac. Sci. Technol. B **22**, 2902 (2008).
[8]J. D. Beard and S. N. Gordeev, Nanotechnology **22**, 175303 (2011).
[9]P. Bøggild, T. M. Hansen, C. Tanasa, and F. Grey, Nanotechnology **12**, 331 (2001).
[10]S. Bauerdick, A. Linden, C. Stampfer, T. Helbling, and C. Hierold, J. Vac. Sci. Technol. B **24**, 3144 (2006).
[11]T. Bret, I. Utke, P. Hoffmann, M. Abourida, and P. Doppelt, Microelectron. Eng. **83**, 1482 (2006).
[12]M. Tanaka, M. Shimojo, M. Han, K. Mitsuishi, and K. Furuya, Surf. Interface Anal. **37**, 261 (2005).
[13]L. van Kouwen, A. Botman, and C. W. Hagen, Nano Lett. **9**, 2149 (2009).
[14]W. F. van Dorp, C. W. Hagen, P. A. Crozier, and P. Kruit, Nanotechnology **19**, 225305 (2008).
[15]A. Perentes and P. Hoffmann, Chem. Vap. Deposition **13**, 176 (2007).
[16]A. Perentes, T. Bret, I. Utke, P. Hoffmann, and M. Vaupel, J. Vac. Sci. Technol. B **24**, 587 (2006).
[17]H. D. Wanzenboeck, M. Fischer, R. Svagera, J. Wernisch, and E. Bertagnolli, J. Vac. Sci. Technol. B **24**, 2755 (2006).
[18]S. Lipp, L. Frey, C. Lehrer, B. Frank, E. Demm, S. Pauthner, and H. Ryssel, J. Vac. Sci. Technol. B **14**, 3920 (1996).
[19]L. R. Harriott, A. Wagner, and F. Fritz, J. Vac. Sci. Technol. B **4**, 181 (1986).
[20]A. Weber-Bargioni, A. Schwartzberg, M. Schmidt, B. Harteneck, D. F. Ogletree, P. J. Schuck, and S. Cabrini, Nanotechnology **21**, 065306 (2010).
[21]D. J. Burbridge and S. N. Gordeev, Nanotechnology **20**, 285308 (2009).
[22]M. H. Song and K. Furuya, Sci. Technol. Adv. Mater. **9**, 023002 (2008).
[23]F. Banhart, Philos. Mag. Lett. **69**, 45 (1994).
[24]F. Banhart, Phys. Rev. E **52**, 5156 (1995).
[25]D. C. Joy, "A Database of Electron-Solid Interactions," http://web.utk.edu/~srcutk/htm/interact.htm
[26]T. Bret, I. Utke, A. Bachmann, and P. Hoffmann, Appl. Phys. Lett. **83**, 4005 (2003).
[27]G. D. Danilatos, Adv. Electron. Electron. Phys. **71**, 109 (1988).
[28]B. L. Thiel and M. J. Toth, J. Appl. Phys. **97**, 051101 (2005).
[29]J. Cihlar, Colloids Surf., A **70**, 239 (1992).
[30]A. Perentes and P. Hoffmann, J. Vac. Sci. Technol. B **25**, 2233 (2007).
[31]J. J. L. Mulders, L. M. Belova, and A. Riazanova, Nanotechnology **22**, 055302 (2011).
[32]M. Shimojo, M. Takeguchi, and K. Furuya, Nanotechnology **17**, 3637 (2006).